ELSEVIER

Thermochimica Acta 304/305 (1997) 51–66

thermochimica acta

Specific heat spectroscopy: Origins, status and applications of the 3ω method

Norman O. Birge[a,*], Paul K. Dixon[b], Narayanan Menon[c]

[a] *Dept. of Physics and Astronomy, Michigan State University, E. Lansing MI 48824-1116, USA*
[b] *Dept. of Physics, California State University at San Bernardino, 5500 University Pkwy, San Bernardino CA 92407, USA*
[c] *Dept. of Physics and Astronomy, Univ. of California, 405 Hilgard Ave., Los Angeles CA 90095-1547, USA*

Received 10 August 1996; accepted 21 May 1997

Abstract

We review the technique of 'specific heat spectroscopy,' of Birge and Nagel. The technique, also called the '3ω method' in the literature, is nonadiabatic; it is based on thermal diffusion into a thick sample from a thin metallic film that serves simultaneously as heater and thermometer. Specific heat spectroscopy allows one to measure the dynamic specific heat of a liquid or solid over a frequency range exceeding 6 decades, and simultaneously the thermal conductivity over a more limited frequency range. Designed to study supercooled liquids near the glass transition, specific heat spectroscopy has also been used to study phase transitions and biological systems. © 1997 Elsevier Science B.V.

Keywords: 3ω *method; Specific heat spectroscopy; Glass transition*

1. Introduction

The study of the time-dependent linear response of materials forms an important part of condensed matter physics. Measurements of time-dependent or frequency-dependent susceptibilities, such as the dielectric susceptibility, have been performed at least since the previous century [1], and provide a powerful tool to explore the dynamics of condensed matter systems. Many of the standard frequency-dependent susceptibilities describe the linear response to symmetry-breaking external fields; examples include, in addition to the dielectric susceptibility, the magnetic susceptibility, the dynamic structure factor (accessible by neutron scattering), and the various mechanical compliances. In contrast to these dynamic susceptibilities, thermal variables such as the specific heat were considered to be static, and well-defined only for systems in equilibrium.

The concept of a time- or frequency-dependent specific heat arises naturally in systems where a subset of the degrees of freedom – localized modes, for instance – couple only weakly to the predominant modes responsible for heat conduction. An example is a dilute molecular gas, where the vibrational or rotational degrees of freedom of the molecules couple weakly to sound waves [2]. A more subtle situation is the case where the coupling is not necessarily weak, but where some of the degrees of freedom have a long relaxation time compared to the dominant modes. An example of this type of system is a supercooled liquid near the glass transition [3]. Here the heat-carrying modes are the small-amplitude molecular vibrations that will become the phonons in the glassy state. The

*Corresponding author.

PII S0040-6031(97)00201-3

slow degrees of freedom are molecular rearrangements, which relax on ever longer timescales as the glass transition is approached on cooling. The separation of molecular motions into these two classes is not obvious on a microscopic scale, nevertheless, a supercooled liquid exhibits the separation clearly in a measurement of its time-dependent specific heat.

The first observation of a slow time dependence in the enthalpy absorbed or released by a supercooled liquid was made 60 years ago [4]. More recently, differential scanning calorimetry measurements routinely observe (or, more precisely, are limited by) a slowing down of the enthalpy relaxation near the glass transition. In fact, the glass transition temperature, T_g, is often defined as the temperature where the sample falls out of equilibrium on the time scale of the experiment. A treatment of the frequency-dependent specific heat as a linear-response susceptibility – on the same footing as other dynamic susceptibilities – awaited the work of Birge and Nagel [5–7] and of Christensen [8] in 1985. Christensen used the adiabatic technique of specific heat measurement (see Section 3), hence his measurements were limited to a narrow frequency range. Birge and Nagel wanted to measure the specific heat over as wide a frequency range as possible, for several reasons. First, the relaxation time in a supercooled liquid grows rapidly as the glass transition is approached, so a measurement over a narrow frequency range reveals limited information. It was already known from measurements of the dielectric susceptibility of supercooled liquids that the shape of the relaxation function sometimes changes with temperature, hence the traditional method of data analysing using the assumption of time–temperature superposition [3] is flawed. Second, the static specific heat is intimately connected with the Kauzmann entropy catastrophe [9]. An attempt to determine the static specific heat by extrapolating the frequency-dependent specific heat to zero frequency must rely on measurements over the broadest possible frequency range. And third, it was felt that if a technique for the direct measurement of the frequency-dependent specific heat were ever to achieve general usefulness, a broadly accessible frequency range would be essential.

The technique used by Birge and Nagel, called 'specific heat spectroscopy' (SHS), relies on one-dimensional heat diffusion from a planar heater, used simultaneously as the sample thermometer. Birge and Nagel exploited the fact that the heat diffusion equation maintains its simple form in the frequency domain, even if the specific heat is frequency-dependent. With this method, they achieved a frequency range of 5 decades. A drawback of the original technique is that it measured only the product of the specific heat and thermal conductivity [10]. Since then, the technique has been enhanced and the frequency range extended by Dixon and Nagel [11] and by Menon [12]. In particular, a reliable separation of specific heat and thermal conductivity is now possible, based on measurements from two heaters of different widths. In addition, the accessible frequency range of the technique now exceeds 6 decades.

The layout of the article is as follows: Section 2 contains a discussion of the concept of a dynamic specific heat and its relation to hydrodynamic theory, Section 3 contains a full description of the experimental technique, including the separation of the frequency-dependent specific heat from thermal conductivity, Section 4 discusses some applications of the technique, and Section 5 concludes with a discussion of some open questions and possible future applications.

2. Dynamic specific heat

Consider a material with many degrees of freedom of which a subset relaxes slowly, as discussed in the Introduction. In analogy to other linear response measurements, one can imagine performing a time-domain measurement of the dynamic specific heat. We will assume that the sample is of negligible spatial extent, so that we can ignore for the moment spatial temperature gradients and heat diffusion. In principle, one could apply a temperature step to the sample, and then measure the heat input necessary to maintain that temperature. For practical reasons, it is easier to apply a fixed heat pulse ΔQ to a sample isolated from the thermal bath, and to measure the temperature evolution afterwards. One would then find that the temperature jumps upward nearly instantaneously by an amount $\Delta T = \Delta Q/c_{p\infty}$, where $c_{p\infty}$ is the infinite frequency response of the specific heat due to the fast degrees of freedom (phonons, in the case of a liquid or solid). After a long period of time, the slow degrees of

freedom come into equilibrium with the fast ones, and the temperature relaxes back to the value $\Delta T = \Delta Q/c_{p0}$, still above the initial temperature before application of the heat pulse. Here c_{p0} is the equilibrium, thermodynamic specific heat, and $c_{p0} - c_{p\infty}$ is the specific heat of the slowly-relaxing degrees of freedom. Note that $c_{p0} \geq c_{p\infty}$ always. The slow time evolution of the temperature is characterized by a relaxation function, $\Phi(t)$. If the experiment were performed in the frequency domain, one would find a complex, frequency-dependent specific heat of the form [6]:

$$c_p\omega = c_{p\infty} + (c_{p0} - c_{p\infty}) \int_0^\infty -\dot{\Phi}(t)e^{i\omega t}\mathrm{d}t \qquad (1)$$

Thermodynamic derivatives such as specific heat can be related to equilibrium fluctuations by statistical mechanics. The static specific heat of a small system in contact with a reservoir at fixed temperature and pressure is proportional to the entropy fluctuations of the system: $c_p = \langle(\Delta S)^2\rangle/k_B V$, where V is the volume of the system [13]. The frequency-dependent specific heat is then given by linear response theory [14]:

$$c_p(\omega) = \frac{-1}{k_B V} \int_0^\infty \mathrm{d}t \cdot e^{i\omega t} \frac{\mathrm{d}}{\mathrm{d}t} \langle (S(t) - \bar{S})(S(0) - \bar{S})\rangle \qquad (2)$$

where $\bar{S}$ is the average value of the entropy. Eq. (2) is valid only for an infinitely thin sample, where issues of heat flow are irrelevant. For a bulk sample, one should derive the relation between $c_p(\omega)$ and correlation functions from hydrodynamic theory, which takes into account the conservation laws of energy, particle number and momentum. Such a derivation has been performed by Jackle [15,16] and by Gotze and Latz [17], who derive the full set of linearized hydrodynamic equations for a viscous liquid with slow relaxation in both thermal and mechanical variables.

In cases where a set of weakly-coupled, localized modes is not readily identifiable, one might question whether the concept of a frequency-dependent specific heat is sensible, or even necessary, to describe experimental data. Oxtoby objected in principle to the concept of a frequency-dependent specific heat, preferring to describe the experiments in terms of a frequency and wave-vector-dependent thermal conductivity [18]. A more serious concern is whether the measured quantity contains any information that is not already accessible by other experiments, perhaps with less difficulty. Zwanzig pointed out that if there is no frequency dependence to the specific heat at constant volume, c_v, so that the observed frequency dependence in $c_p(\omega)$ comes entirely from the part due to thermal expansion, $c_p - c_v$, then the so-called frequency-dependent specific heat can be completely described by a frequency-dependent longitudinal viscosity, or, equivalently, by a frequency-dependent bulk modulus, $K(\omega)$ [19]. Whether the assumption of Zwanzig is borne out in real systems is a question to be resolved by experiment. Due to the difficulty of measuring c_v, the resolution of this issue would require a quantitative comparison of $c_p(\omega)$ and $K(\omega)$, a comparison that has not been performed [20]. But Jackle has pointed out that from known values of c_p, along with the isothermal compressibility and thermal expansion coefficients near the glass transition, one can deduce that $c_{v0} > c_{v\infty}$ and hence that c_v must exhibit frequency dependence [16]. Thus it appears likely that the assumption of Zwanzig is not valid in real glass-forming liquids.

3. Experimental technique

3.1. Heat diffusion and specific heat measurement methods

A traditional method for the measurement of the specific heat of solid or liquid samples is the adiabatic technique [21], so named because the timescale characterizing thermal relaxation of the sample toward the thermal bath is much longer than the timescale of the measurement. Measurements using the adiabatic technique can be performed either in the time-domain or in the frequency domain [22]. In the former, a heat pulse is absorbed by the sample, and the temperature is measured as a function of time, whereas in the latter, a sinusoidal heat flow is applied and the ac temperature variations are measured with a lock-in amplifier. The adiabatic technique is a powerful technique, with great sensitivity and resolution. For measurements over a large time or frequency range, however, the adiabatic technique has severe limitations. The upper frequency

limit is imposed by the condition that the sample achieve spatial thermal equilibrium in a time much shorter than the measurement time (of order the oscillation period). The lower frequency is limited by the condition that the measurement be faster than the equilibration time of the sample to the external heat bath. Typical organic liquids have very low thermal diffusivities, $\kappa/c_p \approx 10^{-7}\mathrm{m}^2/\mathrm{s}$, where κ is the thermal conductivity, so even with a very thin sample ($d \approx 0.1$ mm) the heat diffusion time across the sample is 0.1 s. (With a much thinner crystalline sample, of course, this time could be considerably shorter. We discuss here the considerations relevant to studies of glass-forming molecular liquids.) A close relative of the adiabatic technique, called the 'relaxation technique' [23], involves measurement of the decay of the sample temperature back to that of the bath. This technique, performed uniquely in the time domain, is subject to the same short-time restriction as the adiabatic method, namely, spatial equilibration of the sample. At long times, any time-dependence of the specific heat would combine with the exponential relaxation of the sample temperature to the bath to produce a complex decay function. Although one could imagine in principle separating the two effects, nobody to our knowledge has attempted such an analysis in practice.

To circumvent the limitations discussed above on the usable frequency range of conventional specific heat measurements, Birge and Nagel used a completely different measurement principle. A thin metal-film resistive heater on a substrate is immersed in the liquid to be studied. (Alternatively, the heater could be deposited directly onto a solid sample.) An ac current at angular frequency ω is passed through the heater [24]:

$$I(t) = I_0\cos(\omega t) \tag{3}$$

The power dissipated in the resistive heater has therefore both a dc component and an ac component at frequency 2ω. The dc component sets up a static temperature gradient in the cell, which must be taken into account in the determination of the absolute sample temperature of the measurement. The ac component causes a temperature oscillation of the heater, of amplitude $T_{2\omega}$ and phase lag φ relative to the power. $T_{2\omega}$ and φ depend both on the geometry of the heater and on the thermal properties of the sample and substrate. If the heater has a temperature coefficient of resistance $\alpha = R^{-1}\mathrm{d}R/\mathrm{d}T$, then the heater resistance also oscillates at frequency 2ω:

$$R(t) = R_0[1 + \alpha T_{2\omega}\cos(2\omega t - \varphi)] \tag{4}$$

By Ohm's Law the voltage across the heater is

$$V(t) = I(t)R(t) = I_0R_0\{\cos(\omega t) + \frac{1}{2}\alpha T_{2\omega}[\cos(\omega t - \varphi) + \cos(3\omega t - \varphi)]\} \tag{5}$$

The last two terms are much smaller than the first; nevertheless the signal at frequency 3ω can be detected with a lock-in amplifier tuned to the third harmonic of the drive signal. (The first term is subtracted by placing the heater in a Wheatstone bridge, to reduce the dynamic range demands on the lock-in amplifier.) The 3ω signal contains information about the thermal properties of the sample through $T_{2\omega}$ and φ, hence the name '3ω method.'

To see exactly what is measured, one must solve the heat diffusion equation in the relevant geometry, with boundary conditions for the heater and the walls of the sample. If the heater is wide and the walls of the cell far away (the precise limits will be discussed in Section 3.4), then the one-dimensional heat diffusion equation is appropriate. In the frequency domain, the equation takes the form:

$$-2i\omega c_p(2\omega)T(x,2\omega) = \kappa\frac{\mathrm{d}^2}{\mathrm{d}x^2}T(x,2\omega) \tag{6}$$

where the actual time-dependence is understood to be $T(x,t) = Re\{T(x,2\omega)e^{-i2\omega t}\}$. The boundary condition at the heater ($x = 0$) is:

$$\kappa\left.\frac{\partial T}{\partial x}\right|_{x=0^-} - \kappa\left.\frac{\partial T}{\partial x}\right|_{x=0^+} = j_q \tag{7}$$

where j_q is the sinusoidal heat flux, equal to the ac power per area dissipated in the heater. The solutions to Eqs. (1) and (2) for the temperature variation at the heater is:

$$T_{2\omega}e^{i\varphi} \equiv T(0,2\omega) = \frac{j_q e^{i\pi/4}}{\sqrt{2\omega}\left(\sqrt{c_p\kappa} + \sqrt{c_{ps}\kappa_s}\right)} \tag{8}$$

where c_p, κ, c_{ps}, and κ_s, are the (possibly frequency-dependent) specific heat and thermal conductivity of

the sample and of the substrate, respectively. The experiment must be performed first with an empty sample cell to determine the product $c_{ps}\kappa_s$ as a function of temperature. Those results are then subtracted from the data taken with the sample, to extract the desired information. Eq. (8) shows that the one-dimensional geometry provides information only on the product $c_p\kappa$, and not on either quantity alone. The method to separate of c_p and κ exploits deviations from the perfect one-dimensional geometry, using two heaters of different widths. The details will be described in Section 3.4.

It is clear that the combination of thermal parameters measured by the experiment depends on the heater and sample geometry. Interestingly, the 3ω method itself (i.e. use of a common heater/thermometer and detection at the third harmonic of the drive current) was invented long ago to study the thermal properties of the heaters themselves, that is, metal or semiconducting wires [25–27]. The method appears to have been forgotten until it was reinvented by Birge and Nagel to study supercooled liquids [28]. These authors also noted that for a narrow heater (a wire), the signal depends more on the thermal conductivity of the surrounding medium, and less on the specific heat [6]. Cahill and Pohl [29] further developed the 3ω method with a narrow heater and showed that the method has many advantages over traditional methods of measuring thermal conductivity. (It was these authors who coined the name, '3ω method.') One could also use the 3ω detection method in an adiabatic specific heat measurement. In doing so, one would gain the advantage of reducing the number of addenda to the sample stage, at the cost of a more complex detection circuit.

3.2. Heater design

3.2.1. Heater substrate

If the sample is a liquid, it is necessary to deposit the heater on a solid substrate which must satisfy certain constraints. First, the substrate must be thick compared to the characteristic thermal length Γ (the inverse of the thermal wavevector k) over which the temperature profile decays away from the heater

$$\Gamma = |k|^{-1} = \left(\frac{\kappa_s}{\omega c_s}\right)^{1/2} \tag{9}$$

The temperature profile away from the heater surface ($x = 0$) is given by

$$T(x, 2\omega) = T(0, 2\omega)e^{-(1-i)\frac{x}{\Gamma}} \tag{10}$$

For the lowest frequency ω to be used, the substrate thickness D must be greater than 2Γ for corrections of less than 2% of the temperature at the heater. For a frequency of $f = 0.01$ Hz on a glass substrate with $\kappa_s \sim 1$ J/sKm and $c_{ps} \sim 10^6$ J/Km^3, the thermal length is $\Gamma \sim 4$ mm and a substrate $D = 10$ mm thick will suffice.

The second constraint is that the heater surface be of optical quality. Flatness on the order of a few μm is helpful but not critical; the critical issue is that the surface have a scratch/dig specification of optical quality. Optical windows made of BK-7 proved to be very dependable.

The third feature of a good substrate material is that the product $c_{ps}\kappa_s$ be as small as possible. As Eq. (8) shows, a large value of $c_{ps}\kappa_s$ compared to $c_{p\kappa}$ for the liquid under study will reduce the sensitivity of the measurement to the thermal properties of the liquid. There is a greater variability in κ_s than in c_{ps} among potential substrate materials. One should avoid highly conductive crystalline materials such as sapphire in favor of amorphous materials like glass; this also helps to minimize Γ.

Finally, it might be possible to construct planar heaters on a thin film instead of a thick substrate in which case the thickness must be small compared to the thermal length in the film material at the highest measurement frequency. This would optimize the signal by allowing heat diffusion into the liquid on both sides of the film.

3.2.2. Heater film

The design of heater films has gone through several improvements; the current state of the art is as follows. The first material to be deposited is 3–6 nm of Cr to provide good adhesion to the glass for the overlying layers and to make the heaters durable. The second, critical, layer is 30–40 nm of Ni. The nickel has a relatively high resistivity and a relatively high coefficient of resistivity, $\alpha \sim 0.003$ K^{-1}. High film resistivities are desirable but resistivities greater than 5 Ω/square lead to uneven films and poor heater performance. The final layer to be deposited is

~200 nm of gold to act as low resistance (of 2–5% of the heater resistance) current leads to the nickel heater. Electrical leads are connected to the gold using 60–40 solder above the liquid level; this prevents the contact resistances from contributing to the signal.

3.2.3. Heater geometry and bandwidth limitations

The operating frequency bandwidth of a heater is determined by the thermal properties of the material under study, the electrical properties of the heater film, and the heater dimensions. For a given material under study, the primary variables under the experimentalist's control are the heater dimensions.

The upper frequency limit $2\omega_{max}$ of the operating bandwidth for a heater is determined by the minimum measurable signal V_{3min} given the noise in the electronics and the desired signal-to-noise ratio. Typical values of V_{3min} are on the order of 1 μV. As Eqs. (5) and (8) show, the magnitude of the signal V_3 is

$$|V_3| = \frac{1}{2} I_0 R_0 \alpha |T(0, 2\omega)| \tag{11}$$

The amplitude of the temperature oscillation (8) can be written as

$$|T(0, 2\omega)| = \frac{j_q}{\sqrt{2\omega}} |Z| \tag{12}$$

if we define the thermal impedance Z as

$$Z = \frac{e^{i\pi/4}}{\sqrt{c_{ps}\kappa_s} + \sqrt{c_p \kappa}} \tag{13}$$

Note that Z is determined purely by the thermal properties of the substrate and sample; we will assume that it is a given quantity in this analysis. The quantity j_q is the power per unit area in the heater; $j_q = P_0/A$. Assuming a rectangular heater of resistance per square R_{sq}, dimensions L and W as shown in Fig. 1(a), and heater power $P_0 = I_0^2 R_0$ we can then write

$$|V_3| = \frac{\alpha I_0^3 R_{sq}^2 L}{2W^3 \sqrt{2\omega}} |Z| \tag{14}$$

For a given minimum measurable signal V_{3min}, we see that the upper frequency limit depends on the geometric factor as

$$2\omega_{max} \propto \frac{L^2}{W^6} \tag{15}$$

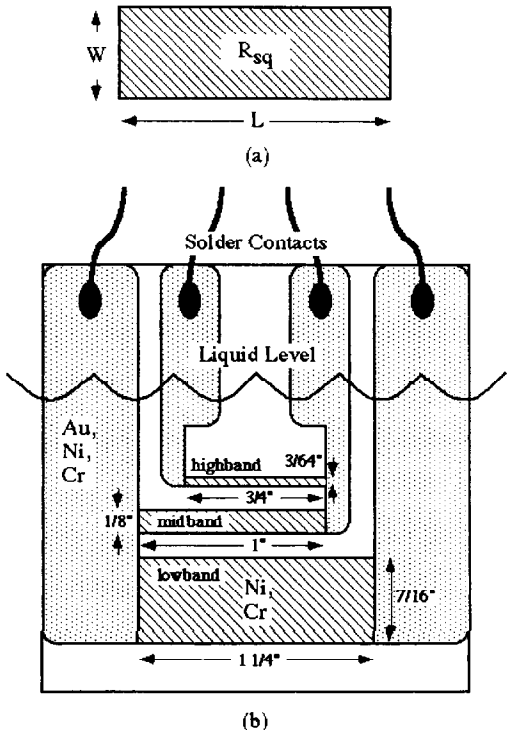

Fig. 1. (a) A schematic of the planar heater geometry: width W, length L and resistance/square R_{sq}. (b) A schematic of the multiband heater design, drawn to scale. The highband, midband, and lowband heaters are shown with their respective dimensions. The lowband heater is relatively far from the lower edge of the glass substrate to avoid any edge effect complications at low frequency. The heaters are made of Ni over Cr. The low resistance leads are made of Au over Ni over Cr.

Clearly, minimizing the heater width is the critical parameter in maximizing $2\omega_{max}$.

The lower frequency limit $2\omega_{min}$ of the operating bandwidth for a heater is determined by the breakdown of the infinite planar heater solution (8) as the thermal length Γ becomes a significant fraction of the heater width W. From Eq. (9), we have $\Gamma \propto 1/\sqrt{\omega}$. As the frequency drops, the ratio Γ/W grows and the finite size effects in the heat diffusion become significant. Assuming that $L > W$, the solution [12] to the heat diffusion equation can be expanded to first order in the ratio Γ/W; the first-order deviation of the phase shift $\Delta\phi$ from the ideal value of $\pi/4$ is

$$\Delta\phi = \frac{\kappa_s + \kappa}{W\sqrt{2\omega}} |Z| \tag{16}$$

Table 1
Multi-band heater dimensions

Heater	Length (mm)	Width (mm)	Nominal (Ω) resistance	$2f_{max}$ (Hz)	$2f_{min}$ (Hz)
Highband	19.1	1.2	40	4000	1
Midband	25.4	3.2	20	50	0.02
Lowband	31.8	11.1	8	5	0.002

A similar expression [12] can be written for $T(0, 2\omega)$. Measurements [12] have shown that Eq. (16) is a good approximation for $\Delta\phi \leq 0.1$ Radians. For a given tolerance on $\Delta\phi$, we see that the low frequency limit scales with geometric factors as

$$2\omega_{min} \propto \frac{1}{W^2}. \tag{17}$$

Maximizing the heater width minimizes $2\omega_{min}$. From Eqs. (15) and (17), we can see that the upper and lower bounds of the operating bandwidth are determined primarily by the heater width W.

The effective bandwidth of a heater is about 3 decades. For broadband measurements, it is necessary to have multiple heaters of overlapping bandwidth on a given substrate. We have designed a multiband heater geometry, Fig. 1(b), that has a collective bandwidth of over 6 decades. The specific values for $2\omega_{max}$ and $2\omega_{min}$ for each heater depend on the material being studied. Most glass formers have similar thermal properties; as an example, we quote the limits [12] for the sample DBP. In Table 1, we quote the operational high frequency, $2f_{max}$, and low frequency, $2f_{min}$, for each heater; note that $\omega = 2\pi f$.

Based upon the constraints discussed above, there is no apparent reason why one could not push the bandwidth to higher frequencies by making a series of heaters with a higher L/W ratio. Unfortunately, at frequencies greater than 10 kHz an additional third harmonic signal generated by a different mechanism becomes the dominant signal. Although it has not been proved, it appears that the mechanism is due to thermally induced acoustic resonances of the heater substrate. The periodic power dissipation into the strip heater induces local thermal expansion oscillations along the length of the heater. If the frequency of the local expansion is near the frequency of an associated resonance of the glass substrate, relatively large oscillations can result. They cause oscillations in the heater resistance and result in a third harmonic signal that masks the smaller SHS term. We have not yet devised a scheme to defeat this spurious signal.

There are limitations to the bandwidth on the low frequency side beyond the constraints of the heater width and substrate thickness. As the temperature of a supercooled liquid is lowered and its characteristic relaxation time τ_c grows, the width in temperature of the transition drops rapidly. For $\tau_c \sim 1$ ms and $\omega_c = 1/\tau_c \sim 1$ mRad/s, transition widths are typically of the order of $\Delta T \sim 1$ K. Accurate measurements in this temperature range require a combination of extremely high temperature stability and low temperature gradients. The necessary temperature stability can be achieved; the gradients are more of a problem. The dc term in the heater power creates a linear temperature gradient ∇T in the sample. For the measurement to be valid, one needs the product $\Gamma\nabla T \ll 1$ K. This leads to impractically small signals since $T(0, 2\omega)$ scales with the power as well.

3.3. Electronics

3.3.1. Wheatstone bridge

SHS measurements are made in a Wheatstone bridge configuration as shown in Fig. 2(a). The source is either a HP3325A function generator or the internal source from a SR830 Digital lock-in amplifier. Both sources have an output impedance $R_0 = 50\ \Omega$ as well as the required high harmonic purity. The output impedance of the source determines the optimal values for other components.

The primary function of the bridge is to null the first harmonic component of V_s across the heater R_s so that the induced third harmonic signal can be measured. The measurement is made differentially across AB (see Fig. 2(a)). The impedance of the right arm of the bridge including the heater is kept comparable to the output impedance of the source to maximize the power

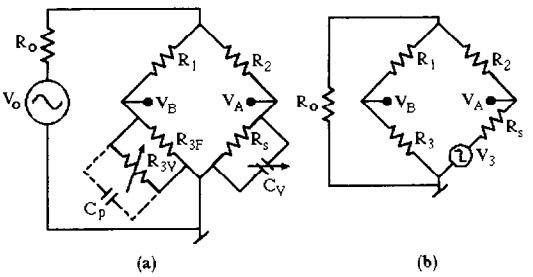

Fig. 2. (a) The circuit diagram for the SHS Wheatstone bridge. The source voltage is V_0, the output resistance of the source is R_0. The right side of the bridge has low resistance, and includes the bias resistance R_2, the heater resistance R_s, and the variable balance capacitor C_v. The left side has high resistance, and includes the resistance R_1, the balance resistance R_{3V} in parallel to R_{3F}, and the parasitic cable capacitance C_p. (b) The effective circuit for the measurement of the third harmonic signal across the points AB. The induced third harmonic voltage in the heater resistance is divided by the bridge.

transfer to the heater, $R_2 + R_s \sim 100\ \Omega$. The resistances in the left arm of the bridge are kept relatively high so as not to draw current. Extremely high values tend to amplify noise contributions and accentuate the effect of parasitic cable capacitances ($C_p \sim 200$ pF) to unbalance the bridge; $R_1 + R_3 \sim 5\ \text{k}\Omega$ is a good working compromise. Wire-wound or metal-film resistors should be used for R_1, R_2, and R_{3F} to minimize the generation of third harmonic signals away from the heater.

The bridge is balanced by varying resistor R_{3V}; we used a Zitech GPIB Decade resistor with the reed relays replaced by mercury-wetted relays to improve durability and reduce noise. It has a range 0–10 kΩ and a resolution of 0.01 Ω. This dynamic range is necessary to balance the source signal $V_0 \sim 10$ V to the required precision of $V_A - V_B \sim 10\ \mu$V. The sensitivity is increased by choosing R_{3F} such that $R_{3\max} = (R_1/R_2)R_{s\max}$.

The parasitic cable capacitance, C_p, induces an out-of-phase component across the bridge; this becomes severe at higher frequencies and requires a variable capacitor C_V placed across R_s. The balance condition requires $R_sC_v = R_3C_p$. Since the ratio R_3/R_s is held constant by the resistance balance condition, the manual variable capacitor C_V need only be adjusted once at the beginning of the experiment; the typical value is $C_V \sim 2$ nF.

The relation between the induced third harmonic voltage in the heater, $V_{3\text{ind}}$, and the measured third harmonic voltage across the bridge, $V_{3\text{meas}}$, is determined by treating the bridge as a voltage divider (see Fig. 2(b)) with the current path through the source V_0 as a short to ground. If the bridge is balanced, the measured signal is

$$V_{3\text{meas}} = \left(\frac{R_2}{R_2 + R_s}\right) V_{3\text{ind}} \tag{18}$$

The measured signal depends upon the power delivered to the heater, Eq. (14) and the divider factor, Eq. (18). Combining the two equations we obtain

$$V_{3\text{meas}} \propto \frac{R_2 R_s^2 V_0^3}{(R_2 + R_s)(R_2 + R_s + R_0)^3} \tag{19}$$

For any given heater resistance R_s, the optimal value for R_2 is $(1/2)R_s$. The signal is maximized for $R_s = (4/3)R_0 = 67\ \Omega$ and $R_2 = (2/3)R_0 = 33\ \Omega$.

3.3.2. *First harmonic measurement*

The first harmonic signal across the bridge can be measured with the same digital lock-in amplifier used to measure the third harmonic signal, but a conventional dual-phase analog lock-in can be used instead. This simplifies continual reconfiguration of the lock-in amplifier settings.

Nulling the first harmonic signal results in a measurement of the heater resistance $R_s(T)$ via $R_{3V}T$. This yields a determination of the necessary quantity $\alpha(T) = (1/R_s(T))\text{d}R_s(T)/\text{d}T$, and it allows for the calibration of the temperature shifts due to the heater power. The difference in the temperature between the heater and the thermometer placed in the sample to control the bath temperature can be determined by doing a series of T scans at different heater power. The deviations ΔT are proportional to the heater power. Due to the extreme sensitivity of the null, the induced shift can be determined with great accuracy. The same approach can be used to determine the temperature lag δT between the temperature control thermometer and the heater due to nonzero scan rates. Furthermore, the measurement of ΔT vs T may be used to determine the temperature at which the sample falls out of equilibrium upon cooling at a given rate. δT is roughly proportional to c_p/κ of the

sample between the heater and the sample can; as the value of c_p drops from the liquid to the glass δT drops accordingly.

3.3.3. Third harmonic measurement

The third harmonic signal across the bridge is measured with a SR830 digital lock-in amplifier. Originally [5–7], the measurement was made with an analog lock-in in conjunction with a frequency tripler. The measurement technique improved with a series of software-based digital lock-in techniques [11,30,31]. The development of commercial digital lock-ins has greatly simplified measurement.

The balanced bridge serves to null the first harmonic term, thus removing a source that could induce a third harmonic response via the nonlinearity of the lock-in pre-amplifier. It also serves to dramatically reduce the third harmonic signals generated in the source. Unfortunately, it produces these two benefits at the expense of a large common-mode signal across the differential inputs to the lock-in. The common-mode rejection ratio of the lock-in is ~80 dB at 1 kHz. For a drive signal of $V_0 \sim 10$ V, this leads to a common-mode signal of ~1 mV compared to a signal strength of $V_{3\text{meas}} \sim 10\,\mu\text{V}$. This is large enough to induce a small third harmonic contribution in the measurement. This contribution can be corrected by switching the inputs to the lock-in and repeating the measurements [12]. The common-mode signal is even upon reversal, $V_A + V_B$, while the true signal is odd, $V_A - V_B$; by taking the difference in the total measurements upon switching, the common-mode contribution can be removed.

There are two approaches to making SHS measurements of supercooled liquids. The preferred approach is to hold T constant and sweep though a series of frequencies. For high accuracy absolute phase measurements [12], the power level has to be held constant as the frequency is changed at the expense of signal strength at higher frequencies.

When the sample is prone to crystallization, the temperature must be scanned to suppress crystallization. The full bandwidth must be measured in a series of overlapping frequency sets. There are two complications to this approach. First, one must perform the analysis in terms of relative phase; as will become apparent in Section 3.4, this makes the separation of c_p and κ more difficult [11]. The second complication is the drift in the first harmonic signal due to the changing temperature during a measurement of the third harmonic signal. A first harmonic signal changing in time has a third harmonic component. If we assume that the first harmonic signal has a component that changes linearly in time:

$$V_1(t) = \beta t \cos(\omega t - \phi') \tag{20}$$

where β and ϕ' and are constants, then the contributions to the third harmonic in-phase and out-of-phase signals are

$$V_{3\text{in}} = \frac{\beta}{4\omega}\sin\phi' \text{ and } V_{3\text{out}} = -\frac{3\beta}{4\omega}\cos\phi' \tag{21}$$

By bracketing the third harmonic measurement with two measurements of the first harmonic signal, the constants β and ϕ' can be determined and the corrections made.

3.4. Separation of specific heat and thermal conductivity

The technique described thus far applies to the case of heat diffusion from an infinite plane heater with negligible thermal capacity and yields the product $c_p\kappa$. The separation of c_p from κ described in this section capitalizes on deviations from the infinite plane limit that depend on the combination c_p/κ through the characteristic thermal length, Γ, defined in Eq. (9) [32].

Eq. (13) for the thermal impedance, Z, is exact in the limit $\Gamma/W \to 0$. The expression to first order in the ratio Γ/W [33] is given for the substrate alone by

$$\begin{aligned} Z &= \frac{e^{i\pi/4}}{\sqrt{c_{ps}\kappa_s}}\left[1 - \frac{\Gamma_s}{W}(1-i)\right] \\ &= \frac{e^{i\pi/4}}{\sqrt{c_{ps}\kappa_s}}[1 - \Delta\phi_s]e^{i\Delta\phi_s} \end{aligned} \tag{22}$$

where

$$\Delta\phi_s \equiv \frac{\Gamma_s}{W} = \frac{1}{W\sqrt{2\omega}}\sqrt{\frac{\kappa_s}{c_{ps}}} \tag{23}$$

and for the substrate and liquid by

$$Z = \frac{e^{i\pi/4}}{\sqrt{c_{ps}\kappa_s} + \sqrt{c_p\kappa}}[1 - \Delta\phi_{SL}]e^{i\Delta\phi_{SL}} \tag{24}$$

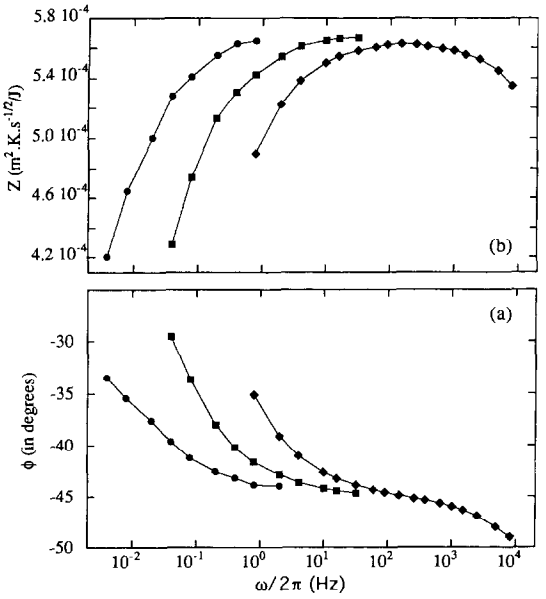

Fig. 3. The frequency response of the low- (●), mid- (□) and high- (◆) band heaters without the liquid displaying the frequency range of infinite plane behavior and the effect of finite size at low frequency: (a) shows the normalized magnitude of the 3ω signal, Z (defined through Eq. (14)) and (b) shows its phase, $\Delta\phi$. In the high-band heater, above 300 Hz, there are deviations from this limit which are speculated to arise from acoustic resonances of the substrate as discussed in Section 3.2.3.

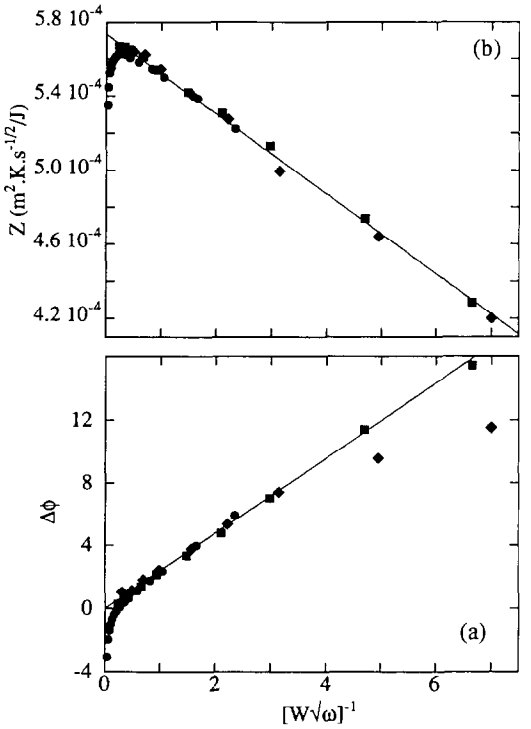

Fig. 4. The frequency and width dependencies of Z and $\Delta\phi$ are plotted in (a) and (b) respectively. Collapse of the data from different heaters is achieved by plotting against $1/(W\sqrt{\omega})$ as predicted by Eqs. (22) and (23). The low frequency asymptotes carry information about $c_p\kappa$ whereas the slopes are determined by κ/c_p.

where

$$\Delta\phi_{SL} = \frac{\kappa_s + \kappa}{\frac{\kappa_s}{\left(\frac{\Gamma_s}{W}\right)} + \frac{\kappa}{\left(\frac{\Gamma}{W}\right)}} = \frac{1}{W\sqrt{2\omega}} \frac{\kappa_s + \kappa}{\sqrt{\frac{\kappa_s}{c_{ps}}\kappa_s} + \sqrt{\frac{\kappa}{c_p}}\kappa} \tag{25}$$

Since the substrate is an amorphous solid, it has no slow modes in the frequency range relevant to this technique. c_{ps} and κ_s (and therefore Γ_s) are non-dispersive and it is straightforward to experimentally test the validity of these expansions by applying Eqs. (22) and (23) to measurements taken with heaters of varying widths at overlapping frequencies. In Fig. 3(a) and Fig. 3(b) the absolute phase and magnitude of the thermal impedance Z (obtained from the magnitude and phase of the third harmonic voltage via Eqs. (11) and (12)) are plotted against log frequency for three heaters with different widths. At frequencies between 0.04 and 16 Hz, there are data points from heaters of two different widths. At high frequencies, where the infinite plane limit is attained for each heater, the phase approaches the value of $\pi/4$ and the magnitude reaches an asymptotic value. The collapse of the low-frequency (finite Γ/W) deviations in accordance with Eqs. (22) and (23) is shown in Fig. 4(a) and (b) by plotting the same data for magnitude and the absolute phase deviation $\Delta\phi_s$ against the quantity $(W\sqrt{2\omega})^{-1}$. The only frequency dependence is through the factor $1/\sqrt{2\omega}$, confirming our expectation that the substrate is non-dispersive in this frequency regime. The slopes of the lines in Fig. 4(a) and (b) yield the ratio κ_s/c_{ps} through Eq. (23) (both the graphs have the same slope within the experimental error of $\sim 2\%$), while the intercept in Fig. 4(a) gives the product $\kappa_s c_{ps}$ through Eq. (13). Thus κ_s and c_{ps} may be independently determined.

Given the success of the first-order expansion in collapsing data from different widths, it may be noted

that data from a single heater would have sufficed to determine κ_s and c_{ps} by the procedure just outlined. This is also true in the presence of the liquid at temperatures where the liquid's thermal properties show no dispersion in the frequency regime of the SHS experiment. If the liquid is dispersive, $\Delta\phi_{sL}$ shows a frequency dependence beyond the factor $1/\sqrt{2\omega}$. To analyze these data, measurements from two heater widths at a given frequency are necessary. Consider data from heaters labelled 1 and 2; we eliminate the finite-size deviation using the known dependence of $\Delta\phi_{sL}$ on heater width to first obtain the asymptotic infinite-plane value:

$$\frac{W_1Z_1 - W_2Z_2}{W_1 - W_2}\exp\left[i\frac{W_1\phi_1 - W_2\phi_2}{W_1 - W_2}\right] = \frac{e^{i\pi/4}}{\sqrt{c_{ps}\kappa_s} + \sqrt{c_p\kappa}} \tag{26}$$

Since κ_s and c_{ps} are already determined, Eq. (26) may be used to find the product $c_p\kappa$. Eq. (25) then yields the ratio c_p/κ. The disadvantage of a direct application of this scheme is that it produces a result with the noise level of the wider heater, which has poorer signal-to-noise ratio at a given frequency. In practice, it was found useful to go through this procedure as a first estimate of the frequency dependence of $\Delta\phi_{sL}$, which is then fit to a smooth function of frequency and used in conjunction with the data from the narrower heater to obtain a better estimate of c_p and κ.

The preceding discussion assumes an absolute measurement of the frequency-dependent phase and magnitude of the third harmonic signal at fixed temperature. This has not been possible until recently [12] due to drifts in the electronics and heater response of earlier configurations of the experiment. Furthermore, as alluded to earlier in the discussion of compensation for drifts in the first harmonic voltage, there are situations where the sample can crystallize and destroy the heater film when held at a fixed temperature. It is possible even under such circumstances to obtain a separation of c_p and κ by the same general ideas [11]. This requires taking temperature scans of sets of two or more frequencies with frequencies overlapping between scans. The liquid can be taken to be non-dispersive at high temperatures and the phase at high temperature is assumed to be the zero phase at all temperatures. A cautionary note to be added here is that any systematic background present in the signal may well be a function of temperature (or time) in which case this assumption will be invalid.

4. Applications

Specific heat spectroscopy has now been applied in a variety of contexts where measurements of the static as well as frequency-dependent specific heat and thermal conductivity are required. In this section, we review selected applications of the technique.

4.1. Supercooled liquids

As discussed in Section 1, Birge and Nagel developed the 3ω method with a view to studying the frequency-dependent specific heat in liquids being cooled toward the glass transition. Since $c_p(\omega)$ carries both the dynamical as well as the thermodynamic information that is central to glass transition, subsequent measurements using this technique bear upon various aspects of our understanding of this problem [34].

One question that has often been asked is whether a particular set of motions is singled out in the slowing dynamics that characterizes the approach to the glassy state. A characteristic frequency of enthalpy relaxation may be associated with the peak in $c_p''(\omega)$ or the crossover in $c_p'(\omega)$. This peak frequency, ν_p, follows the temperature dependence of the viscosity as well as the characteristic frequency obtained from other linear-response measurements (shear modulus, longitudinal modulus, dielectric susceptibility) [12,31,35]. An example is shown in Fig. 5 where these time scales are compared for the supercooled liquid di-*n*-butylphthalate [12]. Since the specific heat weighs all degrees of freedom in the liquid equally, this is evidence that all the slow modes in the liquid are strongly coupled and participate in the dynamical slowing down. The temperature dependence of ν_p is non-Arrhenius to the lowest frequencies attained in this technique. The solid line through the data of Fig. 5 is a fit to the Vogel–Fulcher [36] equation,

$$\nu_p = \nu_0\exp\left[\frac{A}{T - T_0}\right] \tag{27}$$

which implies dynamical arrest ($\nu_p \to 0$) at $T = T_0$. It

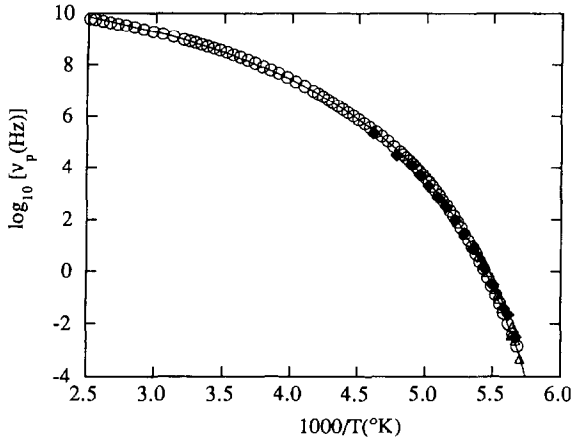

Fig. 5. Logarithm of the relaxation frequency is plotted against $1000/T$ (K) for the supercooled liquid di-*n*-butylphthalate. Data from specific heat spectroscopy (◆) [12] are scaled by the factor $c_{p0}/c_{p\infty}$ to compare with data from dielectric susceptibility (O) [40] and shear modulus (Δ) [44] since the latter two are taken under adiabatic conditions. The solid line is a fit to the Vogel–Fulcher form (Eq. (27)) with $T_0 = 145 \pm 3$ K.

has often been suggested [37] that this non-Arrhenius temperature dependence gives way to Arrhenius temperature dependence at low temperature. Measurements of the dynamic specific heat are especially revealing in this regard since if any motions at all continue to be non-Arrhenius then they will be detected in $c_p(\omega)$.

Low frequency measurements of $c_p(\omega)$ also yield the best estimates of the Kauzmann temperature T_K and suggest a surprising connection between the dynamics and thermodynamic in that $T_0 \approx T_K$ [5,11]. In principle, if $T_0 < T_K$ then we are forced to accept that a Kauzmann situation may be experimentally realized, albeit only by a patient experimentalist. The equality of these two temperatures, however, has not been justified on theoretical grounds and is an experimental matter which further depends on the manner of extrapolation used to obtain these temperatures. Low-frequency SHS data, however, suggest that the Kauzmann paradox is hard to argue away as an extrapolation-dependent artifact since the difference between c_{p0} of the liquid and c_p of the crystal actually increases as T is decreased [12], that is, the entropy of the liquid approaches that of the crystal faster and faster at lower temperature, a fact independent of the extrapolation used to locate T_K.

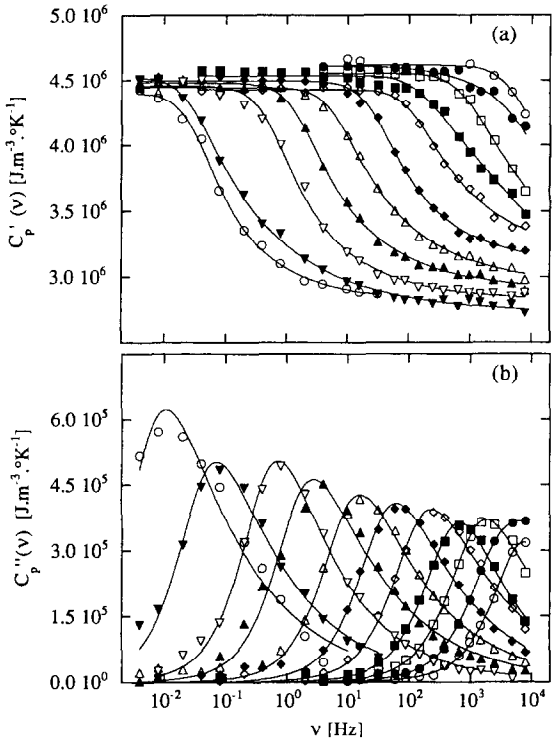

Fig. 6. Real and imaginary parts of $c_p(\nu)$ plotted against $\log_{10}[\nu(Hz)]$ for 11 temperatures from 176.5 to 201 K for the supercooled liquid di-*n*-butylphthalate [12]. The crossover in (a) and the peak in (b) move to lower frequency and become wider at lower T. The lines are fits by a Davidson–Cole form [39].

An example of the full relaxation spectrum is shown in Fig. 6 where $c_p''(\omega)$ and $c_p'(\omega)$ are plotted against $\log_{10}\omega$, again for supercooled di-*n*-butylphthalate [12], for over 6 decades in measuring frequency. As with any other linear susceptibility, c_p'' and c_p' are related by the Kramers–Kronig equations. The spectrum is wider than a Debye relaxation and is asymmetrically stretched toward high frequencies. Several fitting forms have been used to describe the data, of which the most common are the Kohlrausch–Williams–Watts [1,38] form (the frequency-domain representation of a stretched exponential relaxation, $\exp[-(t/\tau)^{\beta}]$) and the Davidson–Cole form $(1/[1+i\omega\tau]^{\beta})$ [39]. These forms describe $c_p''(\omega)$ adequately below the peak frequency, where $c_p''(\omega) \propto \omega$, and for about two decades above the peak frequency, where $c_p''(\omega) \propto \omega^{-\beta}$. At still higher frequencies, a weaker dependence on frequency is found in di-*n*-

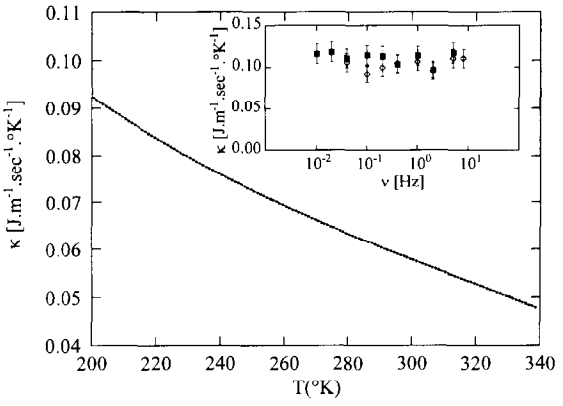

Fig. 7. Thermal conductivity as a function of temperature for the supercooled liquid di-*n*-butylphthalate [12]. κ decreases with increasing temperature. In the inset κ is plotted as a function of frequency at 184 K (squares) and 192 K (diamonds) to show that it is frequency-independent at these temperatures at which c_p is frequency-dependent. We assume this holds at other frequencies, allowing an independent determination of c_p and κ over the entire frequency range shown in Fig. 6.

butylphthalate [12]. Dielectric susceptibility data on a number of supercooled liquids [40], polymers [41] and even on a plastic crystal [42] have revealed an asymptotic high frequency power law behavior whose exponent is connected by a universal material-independent relation to the power law above the peak. Further and more precise measurements are required to determine whether the high-frequency behaviour observed in SHS reflects universalities such as those in the dielectric experiments.

Recent SHS measurements [12,31,43] such as those shown in Fig. 6 also show explicitly that the shape of the relaxation spectrum is temperature-dependent and therefore the assumption of time–temperature superposition does not hold. It is interesting to note, however, that the width of the spectrum does not change much from liquid to liquid. For instance, the full-width at half-maximum of $c_p''(\omega)$, lies between approximately 1.7 and 2.2 decades for glycerol [5], propylene glycol [5], *o*-terphenyl mixtures [11], salol [31], $Ca(NO_3)/KNO_3$ mixtures (CKN) [43] and di-*n*-butylphthalate [12]. Once again, further experiments are necessary to test if this trend is truly general.

As discussed in Section 3, SHS yields an independent determination of thermal conductivity, κ. In all cases measured thus far, κ has been found to be frequency-independent [11,12,43] and appears to be entirely unaffected by the glass transition. Simulations [45] also indicate that heat conduction appears to be decoupled from the slow relaxation times of the liquid. Fig. 7 shows the temperature dependence of κ for di-*n*-butylphthalate [12].

With a complete knowledge of the spectrum of enthalpy relaxations, one may attempt to understand the kinetics associated with the loss of equilibrium on cooling such as is commonly seen in DSC measurements. Jeong et al. have used their SHS measurements on CKN [43] to quantitatively account for the hysteretic nature of the glass transition as one cools and warms the liquid at a fixed rate.

Leyser et al. [46] have made SHS measurements on *o*-terphenyl under pressures of up to about 100 MPa with a view to understanding the role of density and temperature separately. They find that pressure and temperature affect the dynamics rather differently and that equal density states do not give the same relaxation times.

4.2. Phase transitions

There are several potential applications of SHS in the study of phase transitions – it may be used as a precise means of measuring the specific heat and thermal conductivity close to transition as well as a tool to study dynamical critical phenomena where long, hydrodynamic time scales manifest themselves close to the critical point. An interesting example of this is to be found in the experiments of Jeong and coworkers [47,48,49] on the insulating, piezo-electric crystal, K_2HPO_4 (KDP) which has a first-order ferroelectric transition at 120 K. They use a line heater as well as a plane heater directly deposited on a single-crystal sample of KDP to get separate determinations of c_p and κ. (The procedure described in Section 3 works perfectly well for a solid sample, with the added advantage that the background from the substrate is not present to dilute the signal.) The temperature dependence of the thermal conductivity across the transition is used to show the coupling between the acoustic phonons (which are the dominant contribution to κ) and the optical mode whose softening is associated with the ferroelectric transition. They also observe a frequency-dependent c_p at the transition. SHS has also been used to study the ferromagnetic transition in gadolinium [49]. Since Gd is a metal, a

simple modification is required to avoid electrically shorting the heater through the sample – a thin, electrically-insulating layer of SiO of negligible heat capacity is first deposited on the Gd and then the heater is deposited on to this layer.

4.3. Biophysics

SHS affords great promise as a probe of motions of biomolecules and membranes since the dynamics of macromolecules and micron-size molecular assemblages can often lie in the mHz to 10 kHz frequency range which the technique currently provides. Settles et al. [50] have exploited this technique to study the coupling between the function of a protein and its environment. The access of ligands to specific sites on a protein – myoglobin, in the case they study – is not through static channels but is mediated by intramolecular motions which are in turn affected by physical interactions with the solvent. These authors have performed SHS measurements on water–glycerol mixtures with and without horse myoglobin. This choice of solvent gives the facility of substantially changing the viscous damping of protein motions merely by changing temperature rather than by changing solvents or concentrations which could alter specific chemical interactions in an unknown way. They find that the addition of protein into the solution does not substantially change the average relaxation rate of the solvent. However, the relaxation spectrum of the solution is considerably broadened relative to the solvent which leads the authors to conclude that the full time-dependence of the slow modes of the solvent are relevant to the myoglobin motion rather than just the viscosity.

5. Summary

In the relative short history since its inception, Specific Heat Spectroscopy and other 3ω methods derived from it have been applied to a wide range of dynamic and static thermal phenomena. The original objective of the technique was to probe the dynamics of the slow modes in supercooled liquids; that has been the focus of our review. We refer the reader to the other articles in this journal for a review of other 3ω methods.

To date, a rather limited number of glass-forming liquids have been studied with SHS; yet, some intriguing trends have become apparent. In contrast to less precise viscosity measurements, SHS measurements consistently show that the dynamics of supercooled liquids obey the Kauzmann condition, $T_0 > T_K$. Since SHS couples to all the slow modes with equal weight; this makes a much more convincing case than other susceptibilities. Another interesting consistency has shown up in the relaxation width of $c_p(\omega)$. Data from liquids that show great variability in the width as measured by dielectric susceptibility show very little variation in $c_p(\omega)$; This suggests a possible universality. These issues can only be settled by studying a wide range of glass formers.

Using a multiband heater, SHS currently probes more than 6 decades (2 mHz–4 kHz) in the measurement of $c_p\kappa(\omega)$. The separation of $c_p(\omega)$ and $\kappa(\omega)$ can be achieved over a very limited bandwidth. Nonetheless, this analysis has allowed us to prove that κ is independent of frequency; all the dynamics observed in $c_p\kappa(\omega)$ can be attributed to $c_p(\omega)$. It remains unclear whether $c_p(\omega)$ contains information beyond that contained in the compressibility, $K(\omega)$. Simulations [45] indicate that $c_v(\omega)$ does show some dispersion. Very little data exist on the frequency dependence of compressibility; the experiments of Christensen et al. [20] suggest that the relaxation spectrum of $K(\omega)$ differs from $c_p(\omega)$ for glycerol.

There are two obvious avenues for improvement of the technique: extending the bandwidth to higher frequency and improving the sensitivity. Extending the bandwidth will make SHS a more useful susceptibility and help to clarify the relationship between SHS and other susceptibilities. Improving the sensitivity may have more profound implications. Dielectric susceptibility measurements on a wide range of glass-forming liquids have shown that the relaxations can be mapped onto a universal scaling form. For a number of reasons, the key part of this universal spectral shape is the high frequency tail. Unfortunately, the signal-to-noise ratio of SHS is currently about a factor of ten too low to distinguish whether or not $c_p(\omega)$ obeys the scaling form. The other interesting aspect of the glass transition that improved versions of this experiment can shed light on is that of the β of Johari–Goldstein relaxation. It is thought that these modes in the high-temperature liquid state persist all

the way into the glass phase giving rise to the distribution of tunneling levels which are responsible for the linear term in the low-T specific heat of glasses. However, the contributions of these modes to the specific heat of the liquid are small and are presently just beyond the resolution of this technique.

There are technical obstacles in the path of both avenues for improvement. Extending the bandwidth will require overcoming the spurious 3ω signal that dominates the SHS signal at high frequencies. We believe that this spurious signal is due to acoustic resonances of the glass substrate. Defeating this effect will require suppressing the resonances in the substrate or removing the substrate altogether by going to a thin film heater geometry. Even if this is achieved, there is no guarantee that the supercooled liquid itself will not show acoustic resonances immediately below the transition. Improving the signal-to-noise ratio of the technique will require modifications in the substrate as well. There are two choices: make the substrate out of a material with a very low value for $c_{ps}\kappa_s$ or remove the substrate entirely by using a thin film heater. Since developing a thin film heater has the potential to solve both of these problems; it should be the primary technical objective.

Acknowledgements

We should like to thank S.R. Nagel, who introduced all of us to the subject of glass transition and inspired the work reviewed here. N.B. also thanks J.E. Graebner and G. Pollack for useful discussions.

References

[1] R. Kohlrausch, Pogg. Ann. Phys., 91 (1854) 198.
[2] K.F. Herzfeld and T.A. Litivitz, Absorption and Dispersion of Ultrasonic Waves (Academic Press, New York and London, 1959).
[3] For a review of the phenomenology of glasses, see J. Wong and C.A. Angell, Glass: Structure by Spectroscopy (Dekker, New York, 1976). A more recent review is given by M.D. Ediger, C.A. Angell and S.R. Nagel, J. Phys. Chem. 100 (1996) 13200.
[4] P.G. Oblad and R.F. Newton, J. Am. Chem. Soc., 59 (1937) 2495.
[5] N.O. Birge and S.R. Nagel, Phys. Rev. Lett., 54 (1985) 2674.
[6] N.O. Birge, Phys. Rev. B, 34 (1986) 1631.
[7] N.O. Birge and S.R. Nagel, Rev. Sci. Instrum., 58 (1987) 1464.
[8] T. Christensen, J. Phys. (Paris), 46 (1985) C8–635.
[9] W. Kauzmann, Chem. Rev., 43 (1948) 219.
[10] Efforts by Birge (ref. 6) to separate the thermal conductivity from the specific heat by combining the data from a planar heater with those from a second experiment using a wire geometry were not successful in the temperature range where the specific heat was frequency-dependent.
[11] P.K. Dixon and S.R. Nagel, Phys. Rev. Lett., 61 (1988) 341.
[12] N. Menon, J. Chem. Phys., 105 (1996) 5246.
[13] See Chapter 12 of E.M. Lifshitz and L.P. Pitaevskii, Statistical Physics, Vol. 5 of Course of Theoretical Physics by Landau and Lifshitz, (Pergamon Press, Oxford, 1980).
[14] Eq. (2) was written in terms of the enthalpy, rather than the entropy, in ref. 6. That error was then propagated in refs. 12 and 48. (Enthalpy fluctuations include a second term, as shown in ref. 13.) We are grateful to the referee for pointing out this error.
[15] J. Jackle, Z. Physik B, 64 (1986) 41.
[16] J. Jackle, Physica A, 162 (1990) 377.
[17] W. Gotze and A. Latz, J. Phys. Condens. Matter, 1 (1989) 4169.
[18] D.W. Oxtoby, J. Chem. Phys., 85 (1986) 1549.
[19] R. Zwanzig, J. Chem. Phys., 88 (1988) 5381.
[20] Some work along these lines has been done by T. Christensen and N.B. Olsen, Phys. Rev. B, 49 (1994) 15396 and J. Non-Cryst. Solids, 362 (1994) 172–174.
[21] K.D. Maglic, A. Cezairliyan and V.E. Peletsky (Eds.), Compendium of Thermophysical Property Measurement Methods, Vol. 1 (Plenum Press, New York, 1984).
[22] P.F. Sullivan and G. Seidel, Phys. Rev., 173 (1968) 679.
[23] See, for example, R. Bachman et al., Rev. Sci. Instrum., 43 (1972) 205.
[24] The original references (refs. 5–7) put the drive current at frequency $\omega/2$, so that the measurement occurs at frequency ω. We have adopted the different notation in this article in deference to the growing use of the name '3ω method' in the literature.
[25] Ebeling, Ann. d. Phys., 27 (1908) 391.
[26] O.M. Corbini, Physik Z., 11 (1910) 413 and 12 (1911) 292.
[27] L.R. Holland, J. Appl. Phys., 34 (1963) 2350; L.R. Holland and R.C. Smith, J. Appl. Phys., 37 (1966) 4528.
[28] At about the same time as the work of Birge and Nagel, 3ω methods were invented independently for other problems. See for example, M.A. Dubson, Bull. Am. Phys. Soc., 3 (1986) 622.
[29] D.G. Cahill and R.O. Pohl, Phys. Rev. B, 35 (1987) 4067; D.G. Cahill, Rev. Sci. Instrum. 61 (1990) 802.
[30] P.K. Dixon and L. Wu, Rev. Sci. Instrum., 60 (1989) 3329.
[31] P.K. Dixon, Phys. Rev. B, 42 (1990) 8179.
[32] Alternatively, one can choose a completely different geometry such as a thin wire, see Refs. 10 and 48.
[33] H.S. Carslaw and J.C. Jaeger, Conduction of Heat in Solids, (Clarendon, New York, 1959).
[34] Another approach to measuring the product $c_p\kappa(\omega)$ has been applied to supercooled liquids by Büchner and Korpium,

Appl. Phys. B 43 (1987) 29. They use a photoacoustic technique wherein a thin layer of carbon black is laid on the interface between the sample and a gas and illuminated with a laser beam, chopped at the frequency ω. A microphone and lock-in are used to pick up the acoustic signal in the gas.

[35] Y.H. Jeong, S.R. Nagel and S. Bhattacharya, Phys. Rev. A, 34 (1986) 602.

[36] H. Vogel, Phys. Z. 22 (1921) 645; G.S. Fulcher, J. Am. Ceram. Soc. 6 (1926) 339.

[37] C.A. Angell, J. Phys. Chem. Solids, 49 (1988) 863.

[38] G. Williams and D.C. Watts, Trans. Farad. Soc., 66 (1966) 80.

[39] D.W. Davidson and R.H. Cole, J. Chem. Phys., 18 (1950) 1417.

[40] Wu et al., J. Non-Cryst. Solids, 131 (1991) 32; P.K. Dixon et al. Phys. Rev. Lett. 65 (1990) 1108.

[41] N. Menon and S.R. Nagel, Phys. Rev. Lett., 71 (1993) 4095.

[42] D.L. Leslie-Pelecky and N.O. Birge, Phys. Rev. Lett., 72 (1993) 1232.

[43] Y.H. Jeong and I.K. Moon, Phys. Rev., B 52 (1995) 6381.

[44] N. Menon, S.R. Nagel and D.C. Venerus, Phys. Rev. Lett., 73 (1994) 963.

[45] G.S. Grest and S.R. Nagel, J. Phys. Chem., 91 (1987) 4916.

[46] H. Leyser, A. Schulte, W. Doster and W. Petry, Phys. Rev. E, 51 (1995) 5899.

[47] S.M. Lee, S.M. Lin, S.-I. Kwun and Y.H. Jeong, Sol. State. Comm., 88 (1993) 361.

[48] I.K. Moon, Y.H. Jeong and S.-I. Kwun, Rev. Sci. Instr., 67 (1996) 29.

[49] D.H. Jung, T.W. Kwon, D.J. Bae, I.K. Moon and Y.H. Jeong, Meas. Sci. Tech., 3 (1992) 475.

[50] M. Settles, F. Post, D. Muller, A. Schulte and W. Doster, Biophys. Chem., 43 (1992) 107.